Wide Bandwidth Self Calibration

W. D. Cotton March 23, 2010

***Abstract*—This memo describes a self–calibration approach for wide–band interferometric data adapted from VLBI techniques. A demonstration of the method on 7 mm VLBA data is presented. A working implementation is available in Obit.**

***Index Terms*—Wide-band Imaging, Calibration, Interferometry**

I. Introduction

THE next generation of interferometers, e.g. EVLA and ALMA, will derive much of their sensitivity from using a wide bandwidth. Some variation on self–calibration to remove the effects of atmospheric fluctuations will be needed to achieve the high dynamic ranges which are, in principle, possible with these instruments. The traditional self–calibration for narrow–band, well calibrated connected element interferometers solved for only a single phase per antenna; the actual atmospheric fluctuations are a combination of group delay plus dispersive effects whose phase varies with frequency. In order to perform coherent, wide–band self–calibration, these frequency dependent effects need to be taken into account. Such techniques have long been practiced in the VLBI community and these need to be adapted for use with the new generations of instruments. The following memo discusses such a technique and its implementation in the Obit ([1], http://www.cv.nrao.edu/∼bcotton/Obit.html) package.

II. Narrow–band Self–calibration and VLBI

The potential for using the closure properties of phases in arrays of interferometers was first recognized by Jennison in 1958 [2]. The basic physical property used is that the atmospheric and instrumental effects on interferometric phase are largely introduced on an interferometer element basis. This is especially true at radio wavelengths as the entire aperture of the antenna is coherent. Since there are many more combinations of elements (baselines) in an interferometric array than elements, this redundancy can be used to separate source structure from atmospheric effects.

A. Connected Interferometers

Practical implementations for VLBI and connected interferometers were developed beginning in the 1970's [3], [4], [5], [6]. A comprehensive discussion is given in [7]. These techniques were applied to interferometers whose bandwidths were sufficiently small that the variation of atmospheric phase delay with frequency could be ignored and a single phase per antenna and time were sufficient.

National Radio Astronomy Observatory, 520 Edgemont Rd., Charlottesville, VA, 22903 USA email: bcotton@nrao.edu

Manuscript received ; revised

B. VLBI

On VLBI baselines of thousands of km and with independent local oscillators, a single phase per antenna-time was not sufficient so techniques were developed involving the estimation of group delay [8], [9]. These techniques are known collectively as "Fringe fitting". Wide bandwidths have been traditionally employed in the VLBI community explicitly to measure the geometric group delays allowing very accurate determination of the source and antenna geometries.

III. Extension to Wide–bandwidth

With the use of wide bandwidths in connected element interferometers, the variation of atmospheric phase with frequency can no longer be ignored and the group delay estimation techniques of VLBI practice need to be adapted to connected interferometers. In the following, it is implicitly assumed that the isoplanatic patch size is much larger than the primary power pattern of the interferometer elements, i.e. the atmospheric phase error is constant across the field of view. This assumption breaks down for frequencies below about 1 GHz. The following sections consider the effects which contribute to the variation of propagation phase with frequency.

A. Group Delay

At centimeter wavelengths, variation in atmospheric propagation effects are dominated by fluctuations in the water vapor content which is poorly mixed with the other components of the atmosphere. At these wavelengths, water vapor is non-dispersive so its effect can be described as a group delay:

$$\tau \;=\; \frac{1}{2\pi}\frac{\partial\phi}{\partial\nu} \tag{1}$$

where τ is the group delay in seconds, ϕ is the phase in radians and ν is the frequency in Hz. At sub-mm wavelengths, fluctuations in the dry component of the atmosphere can contribute to the group delay. Measurement of group delay is the determination of the linear variation of phase with frequency. The phase contribution of a group delay is:

$$\phi \;=\; \phi_0 \;+\; 2\pi\tau(\nu - \nu_0) \tag{2}$$

where ϕ_0 is the phase at a reference frequency ν_0.

B. Dispersion

At decimeter and meter wavelengths, the ionosphere becomes increasingly important and this medium is dispersive, the phase delay is proportional to the square of the wavelength. At sub-mm wavelengths, water also becomes increasingly dispersive. At long or very short wavelengths, the dispersion of the atmosphere also needs to be taken into account. See

[10] for a discussion of dispersion. Adding a dispersive term d to eq. 2 gives :

$$\phi \ = \ \phi_0 \ + \ 2\pi\tau(\nu - \nu_0) \ + d\nu^{-1} \tag{3}$$

IV. A Wide–band Technique

Since measured phases are all ambiguous by 2π radians, any fitting of a functional form to their variation is nonlinear. Nonlinear least squares solvers generally work much better when fed an initial solution that is relatively close to the best fit result. Any practical technique will have several stages of refinement.

A. Details

Following the technique of [8], an initial estimate of the single band group delay (delay across a single "IF" or "sub-band") can be obtained from the Fourier transform of a set of "stacked" baselines. For observations of a point source at the phase reference position, or a dataset divided by the Fourier transform of the sky model, the phases on each baseline due to source structure are very close to zero and the phases can be considered to be purely antenna based. Assuming a value of zero for all phase–like parameters for a reference antenna, the phases on the baseline between any given antenna, i, and the reference antenna, r;

$$\phi_{ri} \ = \ \phi_i \ - \ \phi_r \ = \ \phi_i$$

is an estimate of the phase for antenna i. Likewise the difference of the baselines involving a third antenna, j, will be an estimate of the phase for antenna i.

$$\phi_{ji} \ - \phi_{jr} \ = \ (\phi_i \ - \ \phi_j \ ) - \ (\phi_r \ - \ \phi_j \ ) \ = \ \phi_i$$

The phases on all such combinations of baselines can be stacked by taking a weighted average of the sines and cosines of the phases. This gives a pseudo–baseline with almost all of the information relating to the phase for antenna i.

The time-lag (group delay) correlation function and the sky frequency visibility spectrum are related by a Fourier transform. Thus, the group delay can be estimated from the location of the peak amplitude of the Fourier transform of the pseudo–baseline visibility spectrum. In the method described here, the pseudo–baseline visibility spectrum is zero padded by a factor of four to increase the resolution in the delay domain. The location is estimated from a moment analysis of the amplitude of the delay domain function and the visibility phase at the peak determined by interpolation of the value of the delay domain function at the position of the peak. This gives the "single–band" group delay and phase at the center of the IF bandpass. This phase needs to be converted to the value at the reference frequency of the IF using the measured delay. The order of the antennas in the baseline must be taken into account and the phases and delays negated if the reference antenna is the second element in the baseline.

One of the major uses of this measured single–band delay is to resolve ambiguities in the multi–band delay (phase gradient between IFs). In the case where the IF bandwidth is much smaller than the IF separation, some care is needed. For reasons that will be apparent later, it is useful to assign a single band delay of zero if the delay is not large enough to move the peak in the delay function at least one cell in the delay function without the zero padding (four cells with the padding). This keeps noise in the single–band delay estimation from causing the multi–band delay estimation from picking the wrong ambiguity but still allow the determination of group delays large enough to have a significant variation in phase across the IF bandpass.

Given the set of IF single band delays and phases, an estimate of the multi–band delay and phase for each antenna can be refined by a number of successive operations; these assume that the IFs are ordered in frequency.

1) The initial guess of the phase is the phase of the first (or reference) IF and the group delay is the average of the single band delays.
2) The group delay can be refined by taking the phase differences of successive pairs of IFs divided by the difference in frequency. The prior estimate of the group delay is used to resolve ambiguities; the phase difference is folded to the range $[-\pi, \pi]$ before determining the delay for each successive pair of IFs. The next estimate of the of group delay is the average of the IF pair values. For the IF pair m, n this is:

$$\Delta\phi^{obs} = \quad \phi^{IFm} - \phi^{IFn} \tag{4}$$
$$\Delta\phi^{prior} = \quad 2\pi\tau^{prior} * (\nu^{IFm} - \nu^{IFn}) \tag{5}$$
$$iturn = \quad integer(0.5 + \tfrac{\Delta\phi^{prior} - \Delta\phi^{obs}}{2\pi}) \tag{6}$$
$$\Delta\phi^{corr} = \quad \Delta\phi^{obs} + iturn \times 2\pi, \tag{7}$$

   fold $\Delta\phi^{corr}$ to the range $[-\pi, \pi]$ then

$$\tau^{mn} \ = \ \frac{\Delta\phi^{corr}}{2\pi(\nu^{IFm} - \nu^{IFn})}$$

   gives the delay estimate from the IF pair m, n.
3) The group delay can be further refined by taking the phase differences pairs of IF differing by two divided by the difference in frequency. The operations are like those in the previous step except the m and n differ by two rather than one. The next estimate of the group delay is the average of the IF pair values.
4) Finally, a refined estimate of the phase at the reference frequency is derived from the average of all IF phases converted to to the reference frequency using the group delay (τ^{prior}) estimated from the previous step.

$$\phi^{prior} = \quad 2\pi\tau^{prior}(\nu^{IFm} - \nu^{IF0}) \tag{8}$$
$$\phi^{obs,m} = \quad \phi^{IFm} - \phi^{prior} \tag{9}$$

   where ν^{IF0} is the reference IF frequency; $\phi^{obs,m}$ is then folded into the range $[-\pi, \pi]$ and becomes the estimate of the phase from IF m. The estimates of ϕ from all IFs are averaged.
5) The total set of antenna IF phases is fitted for phase at the reference frequency and group delay using a non linear least squared fitter starting from the initial phase and group delay estimates. The gsl nonlinear least squares fitter was used for this.

A final determination of the group delay and phase for each antenna is done using a nonlinear least squares fitting of the channel phases. The ultimate precision is obtained from a least squares solution jointly for all antennas and using data from all baselines. In practice, this appears to be much too slow; a test of the gsl solver with a modest amount of simulated data took as much CPU time as the simulated observe time. It is much faster, and nearly as good, to use the pseudo–baseline stacked data for each antenna. For this approach, the gsl nonlinear least squares fitter is adequate.

B. Obit Implementation

Wide-band self–calibration fitting in Obit is implemented in class ObitUVGSolveWB which is derived from class ObitUVGSolve. At present only group delay and phase fitting are implemented but when suitable test data are available, a dispersion term will be added as well. The results are written to an AIPS SN format table; the IF component of the phase is written as the IF phase in the table and all single–band delays are set to the fitted multi-band delay. An eventual dispersive term will also be implemented using the IF phases. This wide-band fitting option can be selected in Calib and any of the Obit imaging tasks which support self–calibration by using sol?Mode = 'DELA'.

V. Verification

Initial testing of the software used simulated data with known calibration errors applied; this calibration was recovered. In order to further test the efficacy of this calibration scheme, a calibrator scan from a 7 mm VLBA dataset was analyzed. This data contained 2 IFs at 42.8 and 43.1 GHz of 4 MHz bandwidth and 128 channels in full polarization. This data is from a spectral line observation so did not use the phase cal system. Instead, a "manual phase cal" was determined from another calibrator scan several hours prior to the test data and used to align the phases and single band delays in both IFs and polarizations and to remove the bulk of the residual multi–band group delay. The remaining phase residuals at other times should be solely those due to varying atmospheric group delay. This was a stringent test of the software as there are only two IFs whose widths are narrow compared to their separation and the data has only moderate SNR. Delays determined from IF phases are ambiguous by about 3.2 nsec.

Residual (multi-band) group delays and phases were determined for each antenna in 12 second solutions. The calibrator source was slightly resolved but a point model was adequate for the calibration; the SNR for most solutions was in the range 20–40. The fitted results are shown in Figure 1. IF averaged data on one baseline with and without these corrections applied are shown in Figure 2. The calibration aligned the phases of the two IFs at near zero phase and flattened them in time. Other baselines had similar results. The coherent multi-band fringe fitting in AIPS could not handle this case and cannot be used for a direct head-to-head comparison. The fitted solutions appears to adequately remove the group delay variations.

VI. Discussion

The adaption of VLBI techniques for wide-band connected interferometers is straightforward enough, however, one aspect of the traditional VLBI approach requires revisiting. The issue is what to do with negative CLEAN components in the sky model used for self–calibration? More precisely, what to do with CLEAN components for a given pixel which sum to a negative value? The traditional self–calibration approach has been to drop such pixels from the sky model as these were generally due to phase errors in the initial (or previous) calibration; Stokes I emission is, by definition, positive.

Tests of high dynamic range self–calibration associated with the testing for [11] show that this is not always appropriate. In a high dynamic range image, the negative summed components may well be a critical part of the sky model which should not be omitted. The sky emission may be positive everywhere but it is continuous whereas the CLEAN components are confined to locations on a grid. Negative values may well be required for a high accuracy sky model; after convolution with the restoring beam, the image will be positive. In the Obit implementation a "noNeg" parameter is added to the user interface where ever detailed control over the usage of negative summed components is needed.

VII. Conclusion

An effective and practical adaptation of the wide-band delay and phase calibration practice used in VLBI observations applied to wide-band connected element interferometers is described. This calibration will be essential to obtain high dynamic range results from EVLA and ALMA observations. A working implementation is available in Obit

References

[1] W. D. Cotton, "Obit: A Development Environment for Astronomical Algorithms," *PASP*, vol. 120, pp. 439–448, 2008.
[2] R. C. Jennison, "A phase sensitive interoferometer technique for the measurment of the Fourier transforms of spatial brightness distributions of small angular extent," *Mon. Not. Roy, Astron Soc.*, vol. 118, p. 276, 1958.
[3] A. C. S. Readhead and P. N. Wilkinson, "The mapping of compact radio sources from VLBI data," *Astrophys. J.*, vol. 223, p. 25, 1978.
[4] W. D. Cotton, "A method of measuring compact structure in radio sources using VLBI observations," *Astron. J.*, vol. 84, p. 1122, 1979.
[5] F. R. Schwab, "Adaptive calibration of radio interferometer data," in *Society of Photo-Optical Instrumentation Engineers (SPIE) Conference Series*, ser. Society of Photo-Optical Instrumentation Engineers (SPIE) Conference Series, W. T. Rhodes, Ed., vol. 231, Jan. 1980, pp. 18–25.
[6] A. E. E. Rogers, "Methods of using closure phases in radio aperture synthesis," in *Society of Photo-Optical Instrumentation Engineers (SPIE) Conference Series*, ser. Society of Photo-Optical Instrumentation Engineers (SPIE) Conference Series, W. T. Rhodes, Ed., vol. 231, Jan. 1980, pp. 10–17.
[7] T. Cornwell and E. Fomalont, "Self–calibration," in *Synthesis Imaging in Radio Astronomy*, ser. ASP Conference Series, R. A. Perley, F. R. Schwab, and A. H. Bridle, Eds., no. 6. Astronomical Society of the Pacific, 1989, pp. 185–197.
[8] F. R. Schwab and W. D. Cotton, "Global fringe search techniques for VLBI," *Astron. J*, vol. 88, pp. 688–694, 1983.
[9] W. Alef and R. W. Porcas, "VLBI fringe-fitting with antenna-based residuals," *Astron. Astrophys.*, vol. 168, pp. 356–368, 1986.
[10] Thompson, A. R. and Moran, J. M. and Swenson, Jr. G. W., *Interferometry and Synthesis in Radio Astronomy, 2nd Edition*, J. M. M. A. R. Thompson and G. W. Swenson, Eds. A Wiley-Interscience publication, Apr. 2001.
[11] W. D. Cotton, "High Dynamic Range Wide Bandwidth Imaging," *Obit Developement Memo Series*, vol. 19, pp. 1–9, 2010.

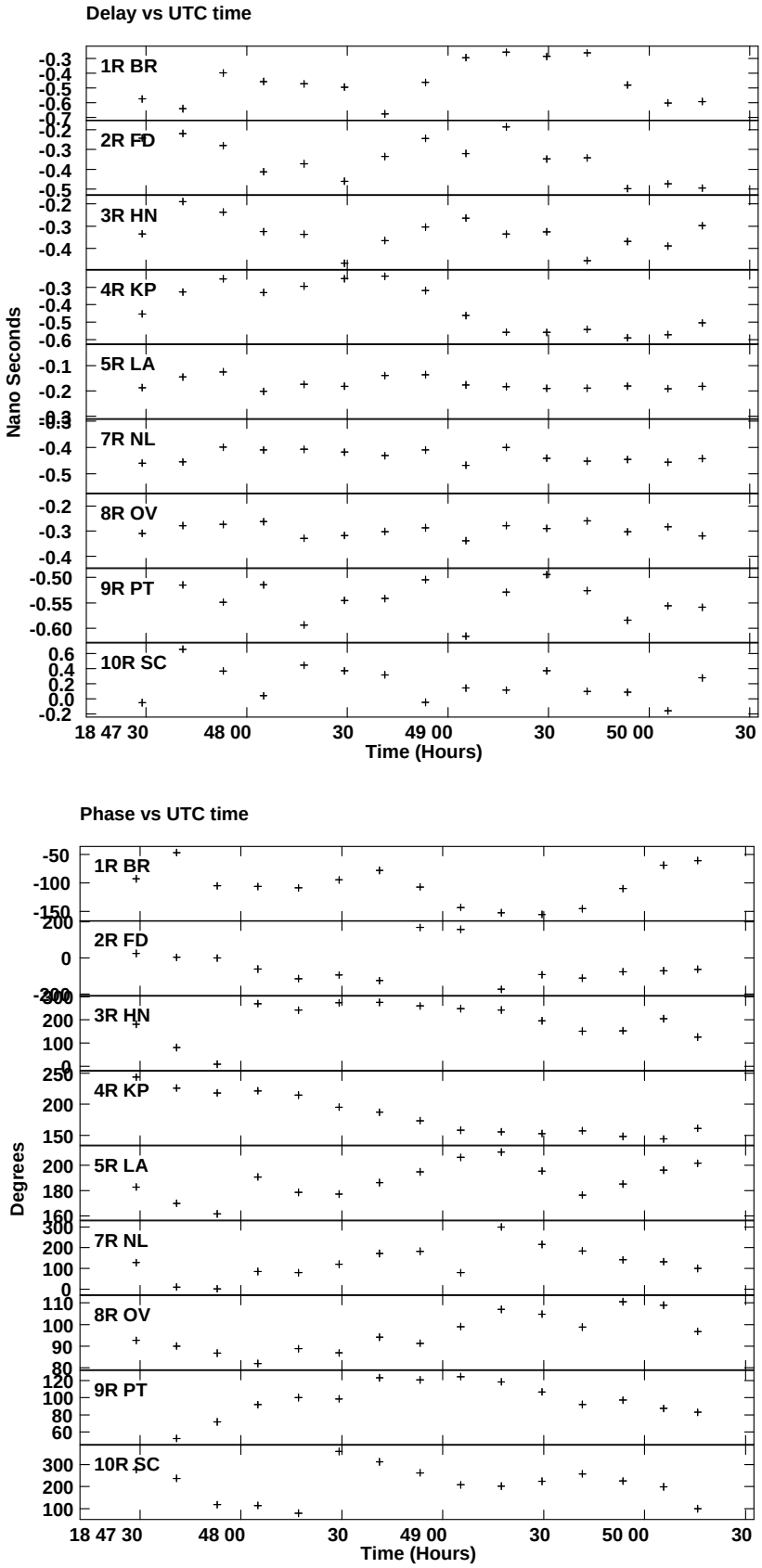

Fig. 1. Fitted group delays and phases from 12 second solutions from a single scan of 7 mm VLBA data. The two IFs are separated by 300 MHz; Mona Kea (MK) was the reference antenna. On the top are the group delays and on the bottom, phases.

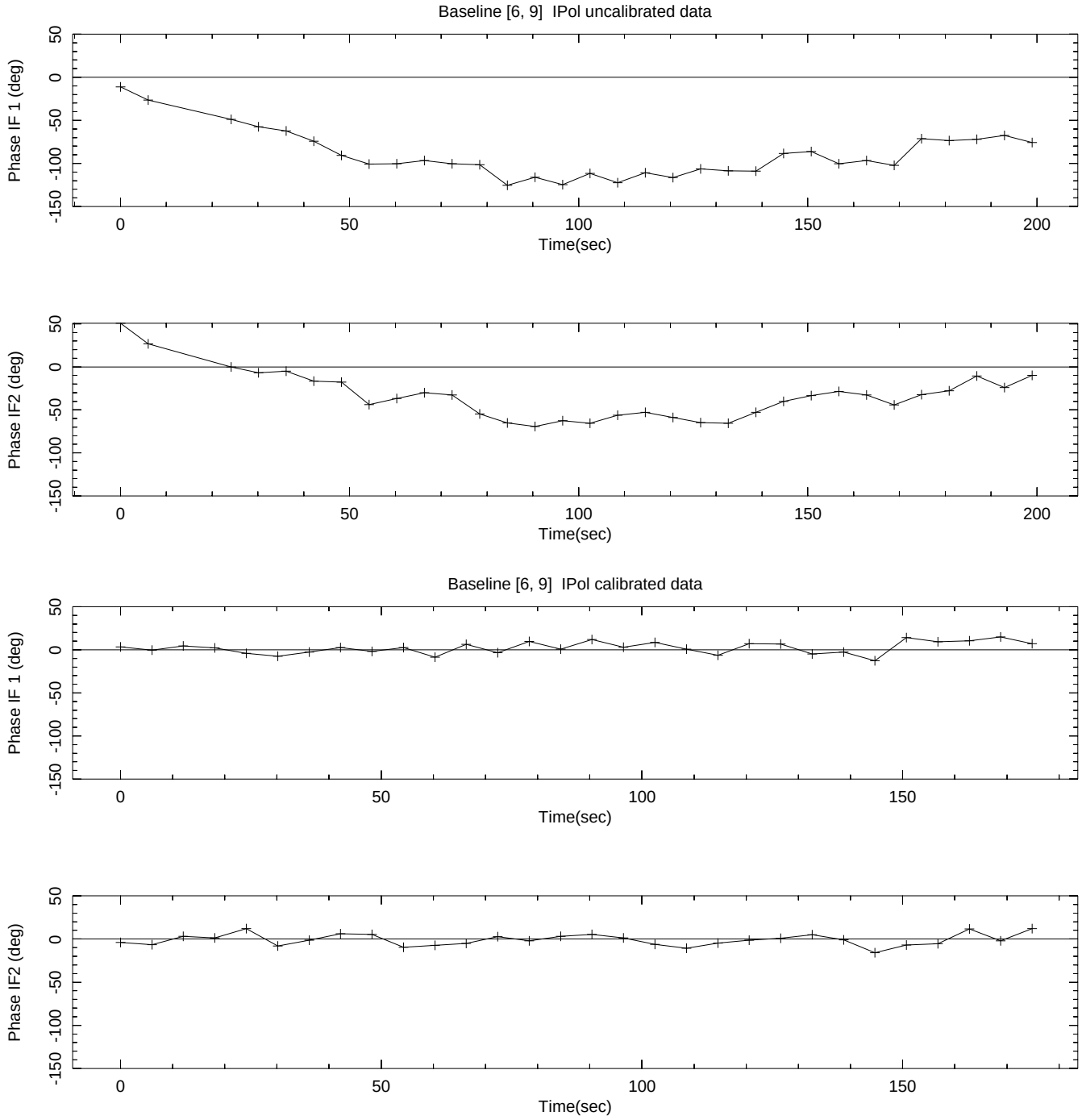

Fig. 2. IF average phase for 6 second data samples on the VLBA baseline from Pie Town, NM to Mona Kea, HI. Upper plots are data with only the “manual phase cal” applied and the lower two plots are after correcting by the values in Figure 1.